



ELSEVIER

Contents lists available at ScienceDirect

Journal of Luminescence

journal homepage: www.elsevier.com/locate/jlumin

Luminescent hybrid materials functionalized with lanthanide ethylenodiaminetetraacetate complexes containing β -diketonate as antenna ligands

Franklin P. Aguiar^a, Israel F. Costa^a, José Geraldo P. Espínola^a, Wagner M. Faustino^a, Jandeilson L. Moura^a, Hermi F. Brito^b, Tiago B. Paolini^b, Maria Cláudia F.C. Felinto^c, Ercules E.S. Teotonio^{a,*}

^a Departamento de Química-Universidade Federal da Paraíba, 58051-970 João Pessoa, PB, Brazil

^b Departamento de Química Fundamental-Instituto de Química da Universidade de São Paulo, 05508-900 São Paulo, SP, Brazil

^c Instituto de Pesquisas energéticas e Nucleares-IPEN, 05508-900 São Paulo, SP, Brazil

ARTICLE INFO

Article history:

Received 30 January 2015

Received in revised form

23 April 2015

Accepted 24 June 2015

Available online 2 July 2015

Keywords:

Lanthanide ions

Hybrid materials

Photoluminescence

Silica gel, β -diketonate

Energy transfer

ABSTRACT

Three organic–inorganic hybrid materials based on silica gel functionalized with (3-aminopropyl)trimethoxysilane (APTS), [3-(2-aminoetilamino)-propil]-trimetoxissilano (DAPTS) and 3-[2-(2-aminoetilamino)etilamino] propiltrimetoxissilano (TAPTS) and subsequently modified with EDTA derivative were prepared by nonhomogeneous route and were then characterized. The resulting materials named SiIXN-EDTA ($X=1$ for APTS, 2 for DAPTS and 3 for TAPTS) were used to obtain new lanthanide Ln^{3+} - β -diketonate ($\text{Ln}^{3+} = \text{Eu}^{3+}$, Gd^{3+} and Tb^{3+}) complexes covalently linked to the functionalized silica gel surfaces (named SiIXN-EDTALn-dik, dik=tta, dbm, bzac and acac). The photophysical properties of the new luminescent materials were investigated and compared with those with similar system presenting water molecules coordinated to the lanthanide ions, SiIXN-EDTALn-H₂O. The SiIXN-EDTAEu-dik and SiIXN-EDTATb-dik systems displayed characteristic red and green luminescence when excited by UV radiation. Furthermore, the quantitative results showed that the emission quantum efficiency (η), experimental intensity parameters Ω_2 and Ω_4 , and Einstein's emission coefficient (A_{0j}) of the SiIXN-EDTAEu-dik materials were largely dependent on the ligands. Based on the luminescence data, the most efficient intramolecular energy transfer processes were found to the SiIXN-EDTAEu-dik (dik: tta and dbm) and SiIXN-EDTATb-acac materials, which exhibited more pure emission colors. These materials are promising red and green phosphors, respectively.

© 2015 Elsevier B.V. All rights reserved.

1. Introduction

In past few years, tremendous interest in the field of material science has been motivated by the development of new compounds that satisfy not only the demands for new and innovative technologies, but also that are consistent with environmental values increasingly required by modern society. In this scenario, the organic–inorganic hybrid materials have achieved a prominent position due to their extensive potential for applications in medical, photochromic, photonics, electronics, catalysis, sensors, biology, environmental, and among others fields [1–6]. Furthermore, the synergistic coupling between organic and inorganic systems at

the molecular scale may go beyond the simple addition and improvement of the properties, but it is possible to obtain novel functional hybrid materials exhibiting new properties.

Among the hybrid organic–inorganic materials, much attention has been aimed to the luminescent systems in particularly those ones based on trivalent lanthanide ions (Ln^{3+}). The recent impacts in this area have been reported in a number of critical reviews ranging from the synthesis strategies and photophysical properties to applications [7–11]. These metal ions are well known by their unique spectroscopic and magnetic properties that are derived from the intrinsic peculiarity of the $[\text{Xe}]4f^N$ electronic configuration, where $N=1-14$. Many of the photophysical (narrow absorption and emission bands) and chemical (predominant ionic bonds) properties are consequences of the shielding effect of the 4f electrons from chemical environment by the 5s² and 5p⁶ electrons. These ligand field interactions relax the parity forbidden nature of the intraconfigurational-4f^N transitions only weakly, resulting in

* Corresponding author. Tel.: +55 83 3216 7591; fax: +55 83 3216 7437.

E-mail addresses: teotonioees@quimica.ufpb.br, ercteot@gmail.com (E.E.S. Teotonio).

absorption bands with strength oscillator values in the order of 10^{-6} . However, in order to obtain highly luminescent lanthanide compounds taking advantages of the other spectroscopic properties of the Ln^{3+} ions (narrow bandwidth, long-lived emission, etc), the low absorption intrinsic of the $4f^N$ transition has been overcome by the “antenna effect”, in which chromophore ligands absorb the excitation energy and transfer it to the Ln^{3+} ion. Consequently, the resulting materials may exhibit high values of luminescence quantum yields [12–14].

In order to prepare organic–inorganic hybrids immobilized lanthanide complexes based on silica gel, different synthetical strategies such as physical doping, sol–gel and postsynthetic methods have been used. In the first case, the luminescent complexes are either introduced into a host mesoporous material or simply impregnated on silica gel surface [15]. However, this method presents the disadvantages of nonhomogeneous distribution and leaching of the complexes when the hybrid system is washed with solvents. In the sol–gel method, the lanthanide ions may be directly incorporated in the system in which hydrolysis of metallic alkoxides without organic group are performed. In another sol–gel path, the silylating agent is previously modified with the functional ligand group that is followed by the polycondensation stage. The advantages of sol–gel methods are low-cost and the possibility to obtain transparent films or monoliths. On the other hand, in the postsynthesis method silica gel surface is firstly functionalized with the silylating agent resulting in hybrid materials which undergo subsequent immobilization reaction with ligand molecules. Only after that, either the lanthanide ions or their complexes are adsorbed on the organically modified surface, obtaining luminescent coordination compounds covalently linked on the inorganic system. This method presents the advantage of providing more homogenous ligand sites for the central metal ions. In a general mode, it has been also demonstrated that both nature of the silylating agents and the supporting materials modify the metal ion adsorption capacity on the surface of the hybrid materials [16].

Luminescent hybrid materials based on functionalized aminopolycarboxylate ligands have gained attention mainly due to higher stability of their metal transition and trivalent lanthanide complexes on the solid surface. In this vein, ethylenediaminetetraacetate (EDTA) and diethylenetriaminepentaacetate (DTPA) derivate ligands have received particular attention. These ligands have been immobilized on both organic (chitosan, polyamine composites, polystyrene, etc) [17–21] and inorganic [22–27] supports by using different preparation routes, producing new adsorbent materials with high metal ion adsorption capacity and short equilibrium time [22]. Furthermore, they also acted as additional coordinating ligands when other species were firstly functionalized on the matrices [27].

Wenzel and co-workers investigated Tb^{3+} -aminopolycarboxylate (EDTA and DTPA) complexes immobilized on silica gel as solid-phase for detection of different carboxylic acids in liquid chromatography [26]. According to that study, Tb -EDTA phase is more sensitive for the detection of chelating compounds, probably due to more accessible coordination sphere. More recently, luminescent organic–inorganic hybrid materials containing Ln^{3+} -complexes with modified EDTA and DTPA have been prepared via sol–gel method using tetraethylorthosilicate (TEOS) as a condenser agent [28]. In this case, the luminescence from the intraconfigurational-4f transitions has been described as a result of the energy transfer from the matrix to the Ln^{3+} ion. On the other hand, no luminescence chromophore sensitizer ligand has been used and all materials containing Tb^{3+} ion exhibit high luminescence from the host materials. A series of bifunctional luminescence and magnetic resonance imaging (MRI) contrast agent hybrid materials based on immobilized 2-thenyltrifluoroacetone (TIA) silica microspheres containing Ln^{3+} -EDTA complexes ($\text{Ln}^{3+} = \text{Eu}^{3+}, \text{Gd}^{3+}$

and Tb^{3+}) were also prepared by sol–gel process [27]. However, the Eu^{3+} compounds show low values of luminescence quantum efficiency ($\eta < 20\%$).

As compared with other polycarboxylate ligands, in the Ln -EDTA complexes the central metal ion is not efficiently encapsulated by the aminopolycarboxylic ligands [29–31]. Furthermore, the reaction of dianhydride (or mono-anhydride) of EDTA with amine moieties may decrease the coordination ability of the EDTA ligand due to the conversion of carboxylate group into an amide one. In this case, the first coordination sphere of the lanthanide ion is generally saturated with water or solvent molecules which act as efficient luminescence quenchers, mainly for Eu^{3+} -complexes. However, these ligands may be substituted by another kind of ligand in order to obtain new functional materials. Wang and co-workers immobilized EDTA-europium complexes covalently on zeolite core–shell composites in which dipicolinic acid (DPA) was used as a sensitizer for Eu^{3+} ion luminescence. [32]

The present work reports on the preparation, characterization and photoluminescent study of new organic–inorganic hybrid materials based on (3-aminopropyl)trimethoxysilane (APTS), [3-(2-aminoetilamino)-propil]-trimetoxissilano (DAPTS) and 3-[2-(2-aminoetilamino)etilamino] propiltrimetoxysilane (TAPTS) functionalized silica gel, containing covalently linked Ln -EDTA complexes ($\text{Ln} = \text{Eu}^{3+}, \text{Gd}^{3+}$ and Tb^{3+}). In order to overcome the low molar absorptivity coefficients ($\epsilon \sim 10^{-1} \text{ L mol}^{-1} \text{ cm}^{-1}$) assigned to the intraconfigurational-4f transitions of the trivalent lanthanide ions, additional β -diketonate ligands (tta, dbm, bzac and acac) have been used as luminescence sensitizers. In this case, the functional materials were built from five different moieties (Fig. 1): (1) silica gel that acts as support surface; (2) silylating agents that provide reactive sites to binding functional groups on the surface; (3) EDTA that coordinates efficiently to the central metal ion; (4) Ln^{3+} ions that offer unique luminescence properties and (5) β -diketonate ligands that act as *antenna*, which are capable of absorbing and transferring energy efficiently to the Ln^{3+} ions. The photoluminescent properties of these organic–inorganic hybrid materials have been investigated both qualitatively and quantitatively from luminescence data and in terms of the experimental intensity parameters (Ω_2 and Ω_4), Einstein's emission coefficient (A), and quantum emission efficiency (η) of the Eu^{3+} energy levels.

2. Experimental

2.1. Reagents

Lanthanide oxides (Eu_2O_3 , Gd_2O_3 and Tb_4O_7), (3-aminopropyl) trimethoxysilane (APTS), [3-(2-aminoetilamino)-propil]-trimetoxissilano (DAPTS) and 3-[2-(2-aminoetilamino)etilamino] propiltrimetoxysilane (TAPTS), ethylenediaminetetraacetic acid (EDTA), concentrated hydrochloric acid, acetic anhydride, acetic acid, pyridine, sodium bicarbonate, 2-methylpyrrolidone were purchased from Aldrich and used without any previous treatment. Lanthanide chlorides ($\text{LnCl}_3 \cdot 6\text{H}_2\text{O}$) and dianhydride ethylenediamine acetic (DA-EDTA) were prepared from lanthanide oxides and EDTA, respectively, according to the procedure described in the literature [33–35]. Silica gel was previously treated by removing some impurities in suspension and metal traces. In a typical test, silica gel was suspended in a solution of HNO_3 and H_2SO_4 in a proportion of 9:1 during 24 h. It was then filtered, washed with water until neutral pH and dried at 423 K under reduced pressure for at least 24 h.

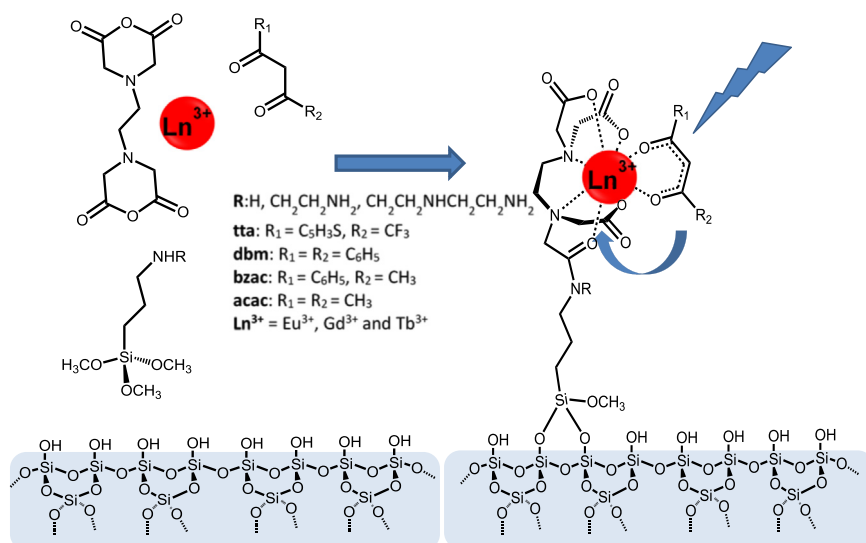


Fig. 1. Scheme showing a proposed structure of the EDTA-Ln-diketonate complexes on the modified silica gel based-hybrid materials.

2.2. Preparation of the materials

2.2.1. Silica-gel functionalization

Silica gel modified with APTS, DAPTS and TAPTS organosilanes were prepared by the standard procedure described in the literature [26]. 20 mmol of APTS, DAPTS or TAPTS organosilane was added to a suspension of 10 g of activated silica gel suspended in 120 mL of toluene at 80 °C mechanically stirred and under dry nitrogen atmosphere. The resulting system was kept under these conditions for 72 h. Thereafter, the mixture was cooled and thoroughly washed with toluene, ethanol and deionized water. The functionalized silica gel was dried under reduced pressure for 12 h at 80 °C. The resulting materials were called Sil1N, Sil2N and Sil3N for silica gel surfaces functionalized with APTS, DAPTS and TAPTS, respectively.

2.2.2. Silica gel modification with ethylenediaminetetraacetate

2, 4 or 6 mmol of EDTA dianhydride dissolved in 80 mL of 2-methylpyrrolidone was added to 10 g of the functionalized Sil1N, Sil2N and Sil3N materials in a three-neck round-bottom flask, respectively. The system under dry nitrogen atmosphere was heated at 60 °C and mechanically stirred for 5 h. The resulting hybrid materials were filtered, thoroughly washed with 2-methylpyrrolidone, deionized water and ethanol. Solid samples were dried under reduced pressure at room temperature for a period of 6 h. The materials were called as Sil1N-EDTA, Sil2N-EDTA and Sil3N-EDTA for the modified materials obtained from the precursors Sil1N, Sil2N and Sil3N, respectively.

2.2.3. Lanthanide complexes on the modified silica gel surface

In order to prepare Na-EDTA on the modified silica gel surfaces, 50 mL of sodium bicarbonate solution with the molar concentrations of 48, 96 and 144 mmol/L were added to 8 g Sil1N-EDTA, Sil2N-EDTA and Sil3N-EDTA, respectively. The resulting suspensions were mechanically stirred for 2 h. Then, the systems were filtered, thoroughly washed with deionized water and ethanol and, dried under reduced pressure. The resulting surfaces were called as Sil1N-EDTANa, Sil2N-EDTANa and Sil3N-EDTANa for surfaces obtained from Sil1N-EDTA, Sil2N-EDTA, Sil3N-EDTA, respectively. For the adsorption of trivalent lanthanide ions, $Ln^{3+} = Eu^{3+}, Gd^{3+}$ and Tb^{3+} on the EDTA modified silica gel surfaces, 25 mL of aqueous solution of lanthanide chloride 80, 160 and 240 mmol/L were added to 1 g of Sil1N-EDTANa, Sil2N-EDTANa and Sil3N-EDTANa samples, respectively. The systems

were mechanically stirred for a period of 24 h at room temperature. Then, the solids were filtered and thoroughly washed with deionized water and ethanol and, finally, dried under reduced pressure. The hybrid materials containing lanthanide complexes were named as Sil1N-EDTALn, Sil2N-EDTALn and Sil3N-EDTALn, where Ln represents the lanthanide ions adsorbed on the surfaces.

2.2.4. Lanthanide complexes containing β -diketonate ligands

25 mL of ethanolic solutions of the β -diketonate ligands (dik=acac, bzac, dbm and tta) were added to 0.1 g of the Sil1N-EDTALn, Sil2N-EDTALn and Sil3N-EDTALn materials at 80, 160 and 240 mmol/L, respectively. The mixtures were kept at room temperature and mechanically stirred for 24 h. After that, the solids were filtered, thoroughly washed with deionized water and ethanol and, dried under reduced pressure. The resulting materials were named as Sil1N-EDTALn-dik, Sil2N-EDTALn-dik and Sil3N-EDTALn-dik.

2.3. Apparatus

FT-IR spectra of the hybrid materials were recorded in the range of 400–4000 cm^{-1} on a Shimadzu FT-IR spectrophotometer model IRPRESTIGE-21 with sample in KBr disks. The percentages of the C, H and N were determined on a Perkin-Elmer model 2400 microanalyzer. The steady-state photoluminescent spectra of the hybrid materials were obtained on a Fluorolog-3 spectrofluorometer (Horiba) in which a 450 W Xenon lamp and a photomultiplier R928P PMT were used as excitation source and detector, respectively. The luminescence decay curves were recorded by using phosphorescence module coupled to this optical instrument.

3. Results and discussion

3.1. Characterization of the hybrid materials

In order to obtain EDTALn complexes covalently binding to the solid surface, silica gel surfaces were functionalized with APTS, DAPTS and TAPTS silylating agents and the resulting materials were modified with ethylenediaminetetraacetic acid dianhydride on which Ln^{3+} ion and diketonate ligands (dik=acac, bzac, dbm and tta) were subsequently coordinated to the metal ion.

Table 1
Elemental analysis data for Si11N, Si11N-EDTA, Si11N-EDTAEu-H₂O and Si11N-EDTAEu-dik hybrid materials, where dik: acac, bzac, dbm and tta.

Material	Carbon		Nitrogen		C/N
	% C	mmol/g	% N	mmol/g	
Si11N	6.67	5.56	2.27	1.62	4.11
Si11N-EDTA	11.03	9.19	2.96	2.11	5.22
Si11N-EDTAEu-H ₂ O	9.24	7.70	3.39	2.42	3.82
Si11N-EDTAEu-tta	10.89	9.08	3.21	2.29	4.75
Si11N-EDTAEu-bzac	10.19	8.49	3.17	2.26	4.50
Si11N-EDTAEu-dbm	10.42	8.68	2.71	1.94	5.38
Si11N-EDTAEu-acac	10.01	8.34	2.83	2.02	4.95

Table 1 presents elemental analysis data of carbon, hydrogen and nitrogen and, Eu³⁺ ion in the Si11N precursor matrices, modified EDTA surfaces (Si11N-EDTA) and also for these surfaces containing Eu³⁺ coordinated by diketonate ligands (Si11N-EDTAEu-dik). The data for similar systems with Si12N and Si13N are presented in Tables S1 and S2. The carbon and nitrogen percentages for Si11N, Si12N and Si13N surfaces show that the functionalization degree, in terms of number of moles per gram of silica gel, present the following trend: Si11N (APTS) > Si12N (DAPTS) > Si13N (TAPTS). On the other hand, the modification trend for these materials with dianhydride of EDTA is the following: Si12N-EDTA > Si11N-EDTA > Si13N-EDTA. This result was estimated based on the difference in the percentage of nitrogen between modified and unmodified precursor materials. A comparison between the number of moles of EDTA groups and the number of organic amine chains anchored in the material indicates that approximately 28%, 15% and 10% aminated chains reacted with the dianhydride of EDTA to obtain the Si11N-EDTA, Si12N-EDTA, and Si13N-EDTA materials, respectively. The lower efficiency in the modification processes on the Si12N and Si13N surfaces, as compared to the Si11N one, may be probable owing to both steric hindrances among longer organic moieties and owing to the interactions between these moieties and the silanols groups on the surface of materials. The β -diketonate ligands coordinated to the Eu³⁺ ions were qualitatively identified by the luminescence sensitizer phenomenon. The hybrid materials containing Tb³⁺ and Gd³⁺ ions exhibited similar behavior as those Eu³⁺-systems.

Figs. S1–S3 present the FT-IR spectra for the hybrid materials, Si1XN, Si1XN-EDTAEu, Si1XN-EDTAEu-dik (where X = 1, 2, or 3 and dik: acac, bzac, dbm or tta). The broad band at around 1085, 796 and 460 cm⁻¹ correspond to the asymmetric stretching, symmetric stretching and planar bending vibrational modes of Si–O–Si groups, respectively [36]. The FT-IR spectra for all hybrid materials clearly show the bands at 3450 cm⁻¹ (O–H, N–H stretching) and 1650 cm⁻¹ (N–H bending), due to the amine groups. Additionally, weak bands around 2930 cm⁻¹ are observed that are assigned to the C–H stretching vibrations from propyl group anchored to the silica gel surface [37].

As compared to FT-IR spectra for Si1XN systems, those ones for Si1XN-EDTAEu exhibit one band at approximately 1380 cm⁻¹ and also show an increase in the intensity of the large band at 1637 cm⁻¹, which are attributed to the antisymmetric and symmetric stretching vibrational modes of the COO⁻ groups. It was not possible to identify the coordination mode of the β -diketonate ligands based on the FT-IR data owing to the low amount of these ligands on the hybrid material surface. Similar behavior has been reported by Tang and co-workers with luminescent lanthanide complexes on attapulgite clay [38].

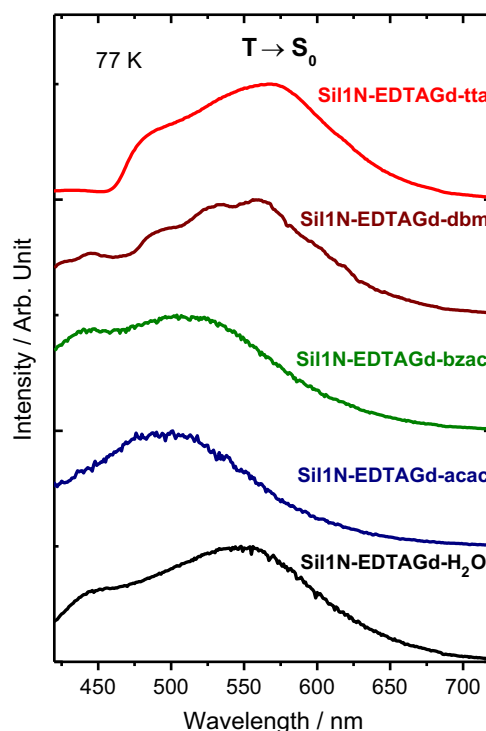


Fig. 2. Emission spectra of the Si11N-EDTAGd-H₂O and Si11N-EDTAGd-dik (dik: tta, dbm, bzac and acac) hybrid materials, recorded at liquid nitrogen temperature under excitation monitored on the matrix (at 350 nm) and antenna ligands (at 370 nm), respectively.

3.2. Photoluminescent properties of the hybrid-material

3.2.1. Photoluminescence of the materials containing Gd³⁺ ion

Luminescence spectra of the hybrid materials containing Gd³⁺ ion recorded at liquid nitrogen temperature under excitation on the singlet–singlet (S₀→S₁) centered ligand transitions show an intense broad band in the spectral range 400–750 nm that is attributed to the phosphorescence intraligand T→S₀ transition from β -diketonate ligands, which overlap the broad bands arising from silica gel matrix (Fig. 2 for Si11N-EDTAGd-dik and Si11N-EDTAGd-H₂O) (See Figs. S4 and S5 for the other materials in the Supplementary information). The latter are better investigated from the luminescence spectra of the hybrid materials without antenna ligands (Si1XN-EDTAGd-H₂O). When the β -diketonate ligands exhibit weak phosphorescence intensities, such as in the systems containing acac and bzac, these bands dominate the emission spectra. The nature of these bands has been assigned to different effects, such as defect centers in the silica gel [39], and the charge transfer process between silicon and oxygen [40], among others [41–43]. In a general mode, the phosphorescence broad bands display a red shift from acac to tta, reflecting the decrease in the energy of the triplet state centered on the diketonate ligands. This result is similar to that observed for isolated complexes (Ligand triplet energies, in cm⁻¹) [44]: acac, 26000 cm⁻¹; bzac, 21460 cm⁻¹; dbm, 20660 cm⁻¹; and tta, 20300 cm⁻¹.

All prepared hybrid materials exhibit intense luminescence when excited with radiation in the spectral range 280–370 nm. However, the luminescent brightness depends on the combination of β -diketonate ligand used as antenna and Ln³⁺ ion (where Ln³⁺: Eu³⁺ and Tb³⁺) coordinated to the EDTA ligand on the silica gel surfaces. For Eu³⁺ ion, the brightest materials are those which contain tta and dbm ligands as luminescence sensitizers, while for Tb³⁺ the brightest systems were found when bzac and acac acted as ligands.

3.2.2. Photoluminescence of the materials containing Eu^{3+} ion

The luminescence sensitizing effect by β -diketonate ligands are better investigated through the excitation spectra under emission monitored on the intraconfigurational $4f-4f$ transitions. Fig. 3 shows excitation spectra for hybrid Si11N-EDTAEu-H₂O and Si11N-EDTAEu-dik materials, by monitoring intensity of the

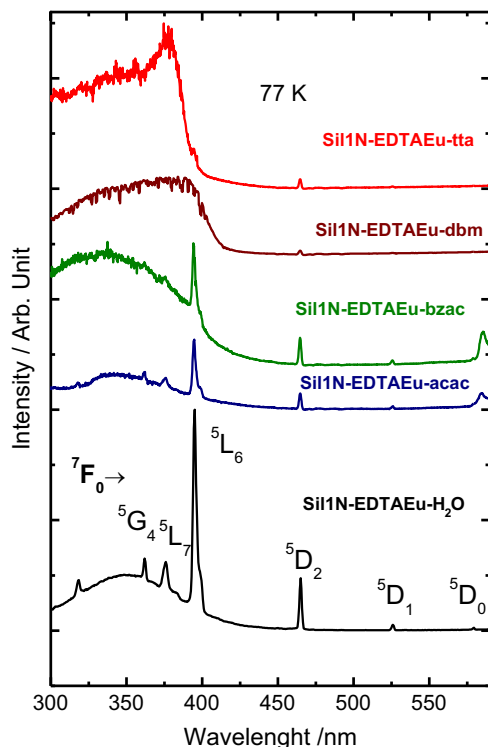


Fig. 3. Excitation spectra for Si11N-EDTAEu-H₂O and Si11N-EDTAEu-dik (dik: tta, dbm, bzac and acac) hybrid materials, recorded at 77 K under emission monitored on the $^5\text{D}_0 \rightarrow ^7\text{F}_2$ hypersensitive transition of the Eu^{3+} at 613 nm.

hypersensitive $^5\text{D}_0 \rightarrow ^7\text{F}_2$ transition at around 613 nm. Figs. S6 and S7 exhibit excitation spectra of the Si2N-EDTAEu-L and Si3N-EDTAEu-L hybrid materials. The excitation spectra for hybrid materials without antenna ligands Si1XN-EDTAEu-H₂O exhibit a broad band from 250 to 450 nm. It is important to report that organically modified silica gel also exhibits low emission intensity in the spectral range 400–630 nm. Consequently, both lanthanide and host materials luminescence are monitored under emission in this interval. These data suggest that broad band in the excitation spectra may be assigned to the host material absorption, which results in a luminescence centered on the modified matrix. The nature of this luminescence has been assigned to different effects [39–43]. Additionally, excitation spectra of Si1XN-EDTA-Eu-H₂O also display narrow bands due to the intraconfigurational- $4f^6$ transitions centered on the Eu^{3+} : $^7\text{F}_0 \rightarrow ^5\text{L}_6$ (394 nm), $^7\text{F}_0 \rightarrow ^5\text{D}_3$ (~448 nm), $^7\text{F}_0 \rightarrow ^5\text{D}_2$ (~464 nm), $^7\text{F}_0 \rightarrow ^5\text{D}_1$ (~525 nm), and $^5\text{D}_0$ (~579 nm), $^7\text{F}_0 \rightarrow ^5\text{D}_4$ (365 nm) and $^7\text{F}_0 \rightarrow ^5\text{G}_2$ (385 nm).

In the excitation spectra for Si1XN-EDTAEu-dik materials, a strong broad band that overlaps the host matrix is displayed in the spectral range 300–400 nm. This band may be attributed to the $\text{S}_0 \rightarrow \text{S}_1$ transition of the diketonate ligands coordinated to the lanthanide ion, indicating that they are acting as luminescence sensitizing for Eu^{3+} ion in these hybrid materials. However, the presence of a weak band due to ligand-to-metal charge transfer (LMCT) may be also overlapped by the most intense bands. Similarly to the excitation spectra for Si1XN-EDTAEu-H₂O hybrid materials, narrow bands due to intraconfigurational transitions centered on Eu^{3+} ion are also observed, but the bands attributed to the $^7\text{F}_0 \rightarrow ^5\text{D}_4$ (365 nm) and $^7\text{F}_0 \rightarrow ^5\text{G}_2$ (385 nm) transitions are observed only in the excitation spectra of the functionalized systems containing acac.

Interestingly, it is also shown that the spectral profiles and the relative intensities of the intraconfigurational transitions depend on the nature of the antenna ligands. In the excitation spectra for hybrid materials containing acac and bzac ligands as luminescence sensitizers, the intraligand broad band, which is assigned to the $\text{S}_0 \rightarrow \text{S}_1$ transition is less intense than that for the $^7\text{F}_0 \rightarrow ^5\text{L}_6$

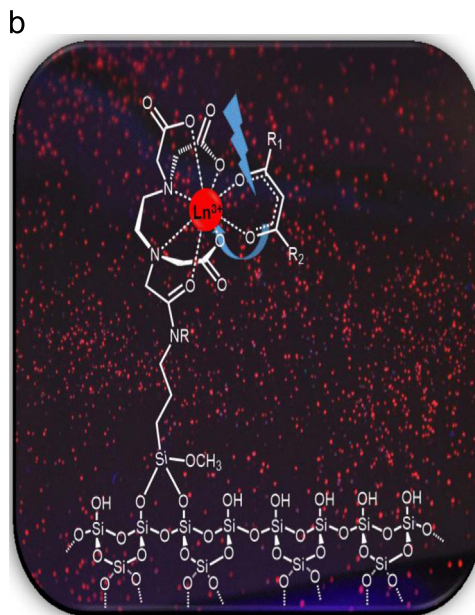
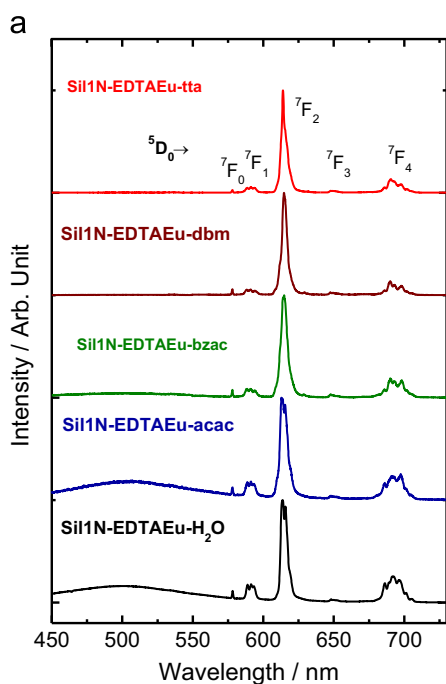


Fig. 4. (a) Emission spectra for the Si11N-EDTAEu-H₂O and Si11N-EDTAEu-dik (dik: tta, dbm, bzac and acac), recorded at liquid nitrogen temperature under emission monitored on the lanthanide ion and $\text{S}_0 \rightarrow \text{S}_1$ ligand transitions at 350 nm, respectively, and (b) Si11N-EDTAEu-tta luminescent material, presenting a proposed structure for EDTA-Ln-diketonate complexes on the surface.

Table 2

Experimental intensity parameters and average lifetime (τ_{av}) of the hybrid materials SiIXN-EDTA-Eu-L (where X=1, 2 and 3 and, L=tta, dbm, bzac, acac and H₂O).

Ligand (L)	A_{rad} (s ⁻¹)	A_{nr} (s ⁻¹)	τ_{av} ($\times 10^{-3}$ s ⁻¹)	A_{total} (s ⁻¹)	Ω_2^a	Ω_4^a	η (%)
Si11N-EDTA-Eu-L							
tta	878	694	0.6362 (0.074)	1572	21.61	11.72	55.8
dbm	975	896	0.5345 (0.056)	1871	25.24	11.99	52.1
bzac	787	918	0.5865 (0.054)	1705	19.39	10.18	46.2
acac	670	800	0.6804 (0.088)	1470	14.59	11.97	45.6
H ₂ O	469	887	0.7425 (0.093)	1347	8.18	10.83	34.1
Si12N-EDTA-Eu-L							
tta	897	679	0.6345 (0.111)	1576	22.08	11.08	59.9
dbm	1038	946	0.5040 (0.059)	1984	27.11	11.52	52.3
bzac	856	688	0.6480 (0.094)	1543	21.08	11.39	55.4
acac	660	890	0.6449 (0.056)	1551	14.39	11.80	42.6
H ₂ O	433	1091	0.6559 (0.055)	1525	8.27	8.87	28.4
Si13N-EDTA-Eu-L							
tta	918	925	0.5424 (0.089)	1844	24.01	9.55	49.8
dbm	938	1229	0.4614 (0.036)	2168	23.74	11.50	43.3
bzac	724	1256	0.5052 (0.031)	1979	17.02	10.67	36.6
acac	629	1125	0.5703 (0.082)	1754	13.93	10.55	35.8
H ₂ O	435	1158	0.6276 (0.061)	1593	8.05	9.45	27.3

^a Ω_2 and Ω_4 ($\times 10^{-20}$ cm²).

transition. On the other hand, when coordinated water molecules in the first coordination sphere are replaced by tta and dbm, the centered ligand transition is more prominent, giving evidence that intramolecular ligand-to-metal energy transfer is more operative than in the similar systems containing acac and bzac ligands. As determined by the phosphorescence spectra of the Gd-hybrid materials, tta and dbm ligands present their low lying triplet excited states in an appropriated relative position to transfer energy efficiently to the excited ⁵D₁ and ⁵D₀ levels of the Eu³⁺ ion [13].

Fig. 4 presents the emission spectra of the Si1N-EDTAEu-L hybrid materials recorded at liquid nitrogen temperature. Similar spectra for Si12N-EDTAEu-L and Si13N-EDTAEu-L ones are presented in Figs. S8 and S9. These spectra exhibit the main intraconfigurational ⁵D₀ → ⁷F_J (J=0, 1, 2, 3 and 4) transitions, presenting the hypersensitive ⁵D₀ → ⁷F₂ as the most intense one. On the bases of the symmetry selection rules, these results indicate that the chemical environments around Eu³⁺ ions in the complexes on the silica gel surfaces belong to C_n, C_{nv} or C_s symmetry group.

Other important feature presented in the emission spectra is the absence of the intense broad band arising from intraligand T → S₀ transition, indicating an efficient Eu³⁺ luminescent sensitization by diketonate ligands, in particular for the systems containing tta and dbm ligands. Fig. 4b shows luminescent solid particles of the Si1N-EDTAEu-tta system and a proposed structure of the hybrid materials. The broad band in the spectral region from 420 to 570 nm is observed for all emission spectra, even in those ones for the hybrid materials without β-diketonate antenna ligands, which may be attributed to the silica gel surface organically functionalized. Furthermore, the relative intensity of this band presents a good correlation with the functionalization degree on the silica gel surface, suggesting that the kind of silylating agents may play an important role in the optical properties of lanthanide hybrid materials.

For Eu³⁺ ion in complexes, a great number of spectroscopic parameters may be determined from the optical data, which provide quantitative information about intensity probabilities of the intraconfigurational-4f⁶ transitions, chemical environment nature, and luminescence efficiency. In this vein, the

photoluminescent properties of the hybrid materials based on silica gel, SiIXN-EDTAEu-dik, were quantified from the experimental values of the radiative (A_{rad}) and nonradiative (A_{nr}) transition probabilities, Judd–Ofelt parameters Ω_λ ($\lambda=2$ and 4) and luminescence quantum efficiency (η) by using the methodology described by Sá and co-workers [45]. In this case, the experimental values of A_{0j} were determined by using the magnetic-dipole ⁵D₀ → ⁷F₁ transition as an internal reference ($A_{01}=0.31 \cdot 10^{-11} \cdot \eta^3 \cdot \sigma^3$) and the value of total radiative rates, A_{rad} , was determined by summing over the A_{0j} rates ($A_{rad}=\sum A_{0j}$):

$$A_{0j} = A_{01} \left(\frac{S_{0j}}{S_{01}} \right) \left(\frac{\sigma_{01}}{\sigma_{0j}} \right) \quad (1)$$

where, S_{0j} and S_{01} are the integrated intensities of the ⁵D₀ → ⁷F_J and ⁵D₀ → ⁷F₁ transitions with σ_{0j} and σ_{01} barycenters, respectively. While the values of Judd–Ofelt Ω_λ parameters were evaluated from the corresponding values of A_{0j} , as follows:

$$\Omega_\lambda = \frac{4e^2\sigma^3 A_{0j}}{3hc^3\chi^3 \langle 7F_J || U^{(\lambda)} || 5D_0 \rangle^2} \quad (2)$$

where σ is the energy of the transition in cm⁻¹, $\chi = \frac{n(n+2)^2}{9}$ is the local field Lorentz correction factor, and $\langle 2S+1L_J || U^{(\lambda)} || 2S+1L_J \rangle$ is the reduced matrix element that was obtained from reference [46]. The value of the refraction index of the media (n) was taken as 1.5. It is important to mention that the values of the A_{06} radiative rate and Ω_6 parameter for hybrid materials were not determined due to the low intensity of the band assigned to the ⁵D₀ → ⁷F₆ transition.

The luminescence intensity decay curves for all the hybrid systems containing Eu³⁺ ion were recorded by monitoring the intensity of the hypersensitive ⁵D₀ → ⁷F₂ transition (around 612 nm) under intraligand S₀ → S₁ excitation. These luminescence decay curves were well adjusted to bi-exponential functions, yielding the values of the pre-exponential terms (A_1 and A_2) that are assigned to the τ_1 and τ_2 components. This bi-exponential adjustment may be assigned to the heterogeneity of the chemical environment around lanthanide ion in the complexes bonded to the silica gel functionalized surface [47]. From these data the total decay rates (A_{total}) were determined by the reciprocal of the average lifetime of the ⁵D₀ level, $A_{total} = 1/\tau_{av} = (A_1\tau_1 + A_2\tau_2)/(A_1\tau_1^2 + A_2\tau_2^2)$.

The experimental values of A_{rad} and A_{total} rates, Ω_λ ($\lambda=2$ and 4) parameters and luminescence quantum efficiency ($\eta=A_{rad}/A_{total}$) are presented in (Table 2). In general mode, the values of A_{rad} present a behavior almost insensible to the nature of the silylating agent, but highly dependent on the ligand that is acting as antenna. The values of A_{rad} rates in the hybrid materials present the following trend: SiIXN-EDTAEu-tta ~ SiIXN-EDTAEu-dbm > SiIXN-EDTAEu-bzac > SiIXN-EDTAEu-acac > SiIXN-EDTAEu-(H₂O). These data reflect the highest hypersensitive nature of the ⁵D₀ → ⁷F₂ transition for the systems containing dbm and tta ligands as antennas.

In contrast to the A_{rad} , the values of A_{nr} are very sensible to the nature of silica gel surface, increasing when the organic chain length becomes larger from Si12N to Si13N surface. These results can be explained by the adsorption of some Eu³⁺ ions via non-functionalized amine groups with EDTA, which coordinate to the metal ion yielding stable complexes on the material surfaces. The lanthanide ions in these coordinating sites could not be totally removed from the materials with the washing procedures, therefore they present solvent or water molecules in their first coordination sphere that contribute to higher luminescence quenching.

The higher values of A_{nr} for the SiIXN-EDTAEu-(H₂O) systems as compared with those ones containing antenna ligands indicate that the multiphonon quenching via high-energy vibrations

modes, such as, $\nu_s(\text{OH})$ and $\nu_{\text{ass}}(\text{OH})$ of the water molecules coordinating to the Eu^{3+} ion is the main operative pathway that depopulates $^5\text{D}_0$ emitting level in these systems. The evidence of this mechanism is given by the significant decrease in the values of A_{rad} when water molecules were substituted by β -diketonate ligands. Although the values of non-radiative rates decrease significantly upon the addition of β -diketonate in the first coordination sphere of the central metal ion, their values still are considerably higher as compared with isolated compounds. This result may be associated with the multiphonon quenching via high-energy $\nu(\text{NH})$ vibration modes of the EDTA moiety that are coordinated to the metal ion.

According to the optical data presented in the Table 2, the values of emission quantum efficiency (η) of the Eu^{3+} complexes increase from 28% to above 40%, when water molecules are substituted by chelating β -diketonate ligands. These results reflect a decrease and an increase of the non-radiative and radiative rates of the luminescent materials, respectively (Table 2). The highest values are found for Si1XN-EDTAEu-tta and Si1XN-EDTAEu-dbm hybrid materials that present the highest values of A_{rad} . However, the values of luminescence quantum efficiency are limited by the presence of NH groups from EDTA moiety in the first coordination sphere, which also play an important role in the Eu^{3+} luminescence quenching.

The values of intensity parameters Ω_2 and Ω_4 obtained for the Si1XN-EDTAEu-(H_2O) $_x$ hybrid materials (Table 2) are close to those ones generally found for Eu^{3+} carboxylate complexes [48, 49]. It is worth noting that upon β -diketonate coordination to Eu^{3+} ion the values of Ω_2 increase significantly for the systems containing tta and dbm ligands. The results suggest that β -diketonate ligands play a relevant role on the chemical environment properties around the Eu^{3+} ion in these hybrid materials such as angular and polarizability changes. On the other hand, the values of Ω_4 increase only slightly, indicating that the chemical environment properties assigned to these parameter are almost insensible to the β -diketonate coordination to the lanthanide ion. Notably, the results presented in Table 2 also show that the silylating group plays a minor role on the chemical environment of the metal ion.

3.2.3. Photoluminescence of the materials containing Tb^{3+} ion

The luminescent properties of the hybrid materials Si1XN-EDTATb-L were only qualitatively investigated based on data obtained from excitation and emission spectra recorded at room and liquid nitrogen temperatures. Considering that no significant spectral differences have been observed among the data registered at these temperatures, here are presented only those spectra recorded at low temperature owing to their better spectral resolution. In Fig. 5 the excitation spectra for the materials Si1N-EDTATb-L recorded between 250 and 520 nm under excitation monitored on the $^5\text{D}_4 \rightarrow ^7\text{F}_5$ transition (around 545 nm) are presented, while Figs. S10 and S11 show the excitation spectra for the Si12N-EDTATb-L and Si13N-EDTATb-L materials. When L is the water molecule (Si1XN-EDTATb-(H_2O) $_x$), these spectra exhibit a broad band which overlaps those ones assigned to the intraconfigurational- $4f^8$ $^7\text{F}_6 \rightarrow ^{2S+1}\text{L}_J$ transitions: $^7\text{F}_6 \rightarrow ^5\text{L}_6$ (339 nm), $^7\text{F}_6 \rightarrow ^5\text{L}_9$ (350 nm), $^7\text{F}_6 \rightarrow ^5\text{L}_{10}$ (369 nm), $^7\text{F}_6 \rightarrow ^5\text{G}_6$ (376 nm), $^7\text{F}_6 \rightarrow ^5\text{D}_3$ (380 nm) and $^7\text{F}_6 \rightarrow ^5\text{D}_4$ (488 nm).

Considering that functionalized host materials also display luminescence around 545 nm, as can be observed in the succeeding emission data, the broad band in those spectra may be assigned to the matrix excitation with subsequent emission. As expected for a system without antenna ligands, the intensities of the $^7\text{F}_6 \rightarrow ^{2S+1}\text{L}_J$ transitions are as higher as those bands centered on the host matrix. On the other hand, excitation spectra of the

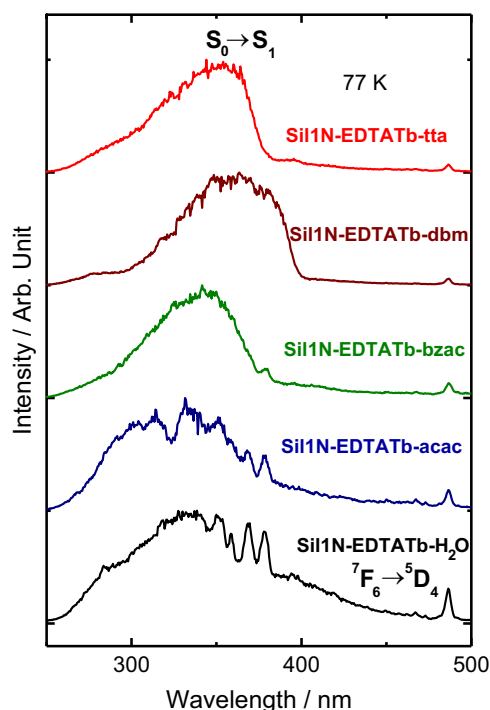


Fig. 5. Excitation spectra of the Si1N-EDTATb- H_2O and Si1N-EDTATb-dik (dik = tta, dbm, bzac and acac) hybrid materials, recorded at 77 K under emission monitored on the $^5\text{D}_4 \rightarrow ^7\text{F}_5$ transition of the Tb^{3+} at 545 nm.

systems containing β -diketonate ligands exhibit broad bands due to the indirect excitation of the Tb^{3+} ions via antenna effect.

For hybrid material Si1XN-EDTATb-acac the highest intense band is that one located at around 320 nm, while for the systems containing the other *antennas* ligands it is located around 350 nm. This result agrees with the highest energy of the singlet excited state (S_1) for acac as compared with the other for tta, dbm and bzac ligands. Although with the lower triplet state energies of both tta and dbm ligands, the excitation data indicate that these ligands are also acting as efficient antennas for Tb^{3+} in the hybrid materials.

Fig. 6 shows the emission spectra of Si1N-EDTATb-L systems registered at liquid nitrogen temperature under excitation around 320 nm (L = acac) and 350 nm (L = tta, dbm and bzac). Similar spectra for Si12N-EDTATb-L and Si13N-EDTATb-L ones are presented in Figs. S12 and S13. The emission spectra for hybrid materials containing tta, dbm, bzac and acac as *antenna* ligands display only intense narrow bands assigned to the intraconfigurational Tb^{3+} transitions $^5\text{D}_4 \rightarrow ^7\text{F}_J$ ($J=0-6$). On the other hand, for Si1XN-EDTATb- H_2O materials the emission spectra show both broad bands due to the functionalized host material. Since that acac is considered as an efficient luminescence sensitizer for Tb^{3+} ion, the low intensity of the intraconfigurational- $4f^8$ transitions in the Si1XN-EDTATb-acac systems may be ascribed to the lower quantity of ligand coordinated to the lanthanide ion.

The chromaticity properties of the hybrid materials were investigated based on the (x , y) CIE coordinates (Commission Internationale de L'Eclairage) which were determined from the photoluminescence data, as described in the reference [50]. Fig. 7, S14 and S15 display CIE diagrams for hybrid materials containing water and β -diketonates ligands. The numeric values of color coordinates are presented in Table 3, S2 and S3. In a general mode, the color coordinate are found in the red and green regions for the hybrid materials containing Eu^{3+} (red region) and Tb^{3+} (green) ions, respectively.

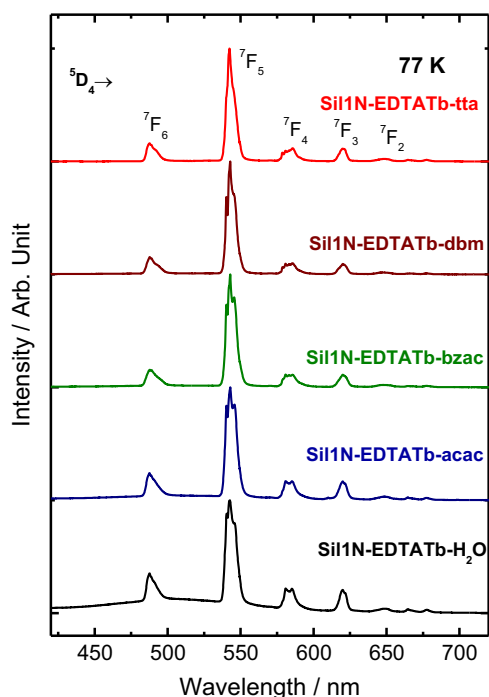


Fig. 6. Emission spectra for the Si11N-EDTATb-H₂O and Si11N-EDTATb-dik (dik: tta, dbm, bzac and acac) recorded at liquid nitrogen temperature under emission monitored on the lanthanide ion and $S_0 \rightarrow S_1$ ligand transitions at 350 nm, respectively.

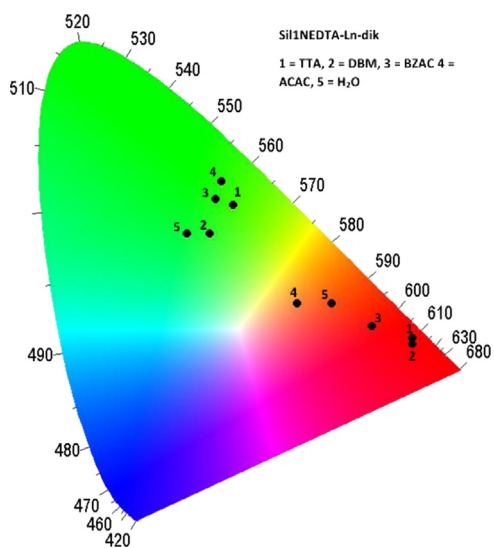


Fig. 7. CIE chromaticity diagram presenting (x,y) color coordinates for the Si11NEDTA-Ln-H₂O and Si11NEDTA-Ln-dik (dik=tta, dbm, bzac and acac) hybrid materials at room temperature under excitation wavelength at 350 nm.

Interestingly, the presence of multiple emitting species (Ln^{3+} ions and matrixes or ligands) contributed to the tunable luminescence colors that depend on the relative intensities between the narrow bands from intraconfigurational- $4f^N$ transitions centered on the lanthanide ions and those ones due to the silica gel matrix or ligands. The hybrid materials containing Eu^{3+} ion with either tta or dbm ligand exhibit monochromatic red color owing to the more operative intramolecular β -diketonate-europium energy transfer. On the other hand, for systems presenting H₂O, bzac and acac orange emission color was observed.

As can be observed, the Si11N-EDTAEu-L hybrid materials present CIE color coordinates similar to the other

Table 3
CIE coordinates of the Eu^{3+} -complexes covalently binding on the silica gel surface functionalized with APTS (Si11N), DAPTS (Si2N) and TAPTS (Si3N).

L	Si11N-EDTA-Eu-L		Si2N-EDTA-Eu-L		Si3N-EDTA-Eu-L	
	x	Y	x	y	x	y
tta	0.65	0.32	0.66	0.31	0.67	0.31
dbm	0.65	0.31	0.67	0.32	0.65	0.32
bzac	0.58	0.34	0.66	0.32	0.59	0.35
acac	0.45	0.38	0.49	0.35	0.42	0.36
H ₂ O	0.51	0.38	0.53	0.38	0.56	0.36

L	Si11N-EDTA-Tb-L		Si2N-EDTA-Tb-L		Si3N-EDTA-Tb-L	
	x	Y	x	Y	x	y
tta	0.34	0.55	0.34	0.52	0.39	0.52
dbm	0.30	0.50	0.32	0.50	0.34	0.50
bzac	0.31	0.56	0.40	0.52	0.35	0.55
acac	0.32	0.59	0.37	0.56	0.35	0.59
H ₂ O	0.26	0.50	0.30	0.49	0.26	0.48

Tb³⁺-compounds reported in literature, presenting x and y values in the intervals of 0.35–0.39 and 0.48–0.59, respectively. For Tb³⁺-hybrid materials, the tunable luminescence colors by changing ligands are lower than those observed in the Si11N-EDTAEu-L materials (L=H₂O, acac, bzac, dbm and tta). This result is expected by considering that the most intense band due to the intraconfigurational transition $^5D_4 \rightarrow ^7F_5$ (~545 nm) centered on the Tb³⁺ ion is less sensible to the chemical environment as compared with the hypersensitive $^5D_0 \rightarrow ^7F_2$ (~612 nm) transition which belong to the Eu^{3+} ion. Furthermore, in Tb³⁺-materials the intraconfigurational transitions $^5D_4 \rightarrow ^7F_6$ (~486 nm, light blue color), $^5D_4 \rightarrow ^7F_4$ (~583 nm, orange color) and $^5D_4 \rightarrow ^7F_3$ (~620 nm, red color) also exhibit significant luminescence intensities.

4. Conclusions

This article shows the preparation of hybrid materials based on silica gel functionalized with three different silylating agents modified with an EDTA derivate by using non-homogeneous route. New luminescent materials have been obtained by adsorbing trivalent lanthanide ions with subsequent coordination of β -diketonate ligands. The photoluminescence properties of the resulting materials are largely dependent on the additional β -diketonate ligand used as luminescence sensitizers. Of particular interest have been the high luminescence efficiencies obtained for hybrid materials containing Eu^{3+} ion and tta or dbm ligands that exhibit values close to 50%. Comparing the values of intensity parameters with those ones for carboxylate and diketonate isolated complexes indicate that both ligands interact efficiently with the central metal ion. The hybrid materials containing Eu^{3+} and Tb³⁺ ions exhibit emission colors in the red and green region of the chromaticity diagram, respectively. However, when ligand is changed tunable emission colors are also observed, which is more significant for hybrid materials presenting Eu^{3+} ion than the Tb³⁺ ion. The luminescence intensities obtained for the novel Eu^{3+} and Tb³⁺ modified silica gel based-hybrid materials suggest that they are promising red and green phosphors, respectively.

Acknowledgments

We thank the Conselho Nacional de Desenvolvimento Científico e Tecnológico (CNPq), and to the Coordenação de Aperfeiçoamento

de Pessoal de Nível Superior (CAPES) for the financial support. We are also grateful to the Instituto Nacional de Ciência e Tecnologia-Nanotecnologia para Marcadores Integrados (INCT-INAMI), PRONEX-FACEPE, Fundação de Amparo à Pesquisa do Estado de São Paulo (FAPESP), and Financiadora de Estudos e Projetos (FINEP).

Appendix A. Supplementary material

Supplementary material associated with this article can be found in the online version at <http://dx.doi.org/10.1016/j.jlumin.2015.06.038>.

References

- [1] C. Sanchez, K.J. Shea, S. Kitagawa, *Chem. Soc. Rev.* 40 (2011) 471.
- [2] C. Sanchez, P. Belleville, M. Popall, L. Nicole, *Chem. Soc. Rev.* 40 (2011) 696.
- [3] P.J. Scully, L. Belancor, J. Bolyo, S. Dzyaderych, J.M. Gimson, R. Fernandez-Lafuente, N. Jaffrezic-Renault, G. Kuncova, V. Matejec, B. O'Kennedy, O. Podrazky, K. Rose, L. Sasek, J.S. Young, *Meas. Sci. Technol.* 18 (2007) 3177.
- [4] S. Dembski, C. Graf, T. Krüger, U. Gbureck, A. Ewald, A. Bock, E. Rühl, *Small* 4 (2008) 1516.
- [5] R. Houbertz, L. Frohlich, M. Popall, U. Streppel, P. Dannberg, A. Brauer, J. Serbin, B.N. Chichkov, *Adv. Eng. Mater.* 5 (2003) 551.
- [6] R. Houbertz, *Appl. Surf. Sci.* 247 (2005) 504.
- [7] L.D. Carlos, R.A.S. Ferreira, V.Z. Bermudez, S.J.L. Ribeiro, *Adv. Mater.* 21 (2009) 509.
- [8] P. Escribano, B.J. Lopez, J.P. Aragó, E. Cordoncillo, B. Viana, C. Sanchez, *J. Mater. Chem.* 18 (2008) 23.
- [9] B. Yan, *RSC Adv.* 2 (2012) 9304.
- [10] J. Feng, H. Zhang, *Chem. Soc. Rev.* 42 (2013) 387.
- [11] L.D. Carlos, R.A.S. Ferreira, V.Z. Bermudez, B.J. López, P. Escribano, *Chem. Soc. Rev.* 40 (2011) 536.
- [12] V.S. Sastri, J.C.G. Bunzli, V.R. Rao, *Modern Aspects of Rare Earths and Their Complexes*, Hardcover, Elsevier Science Publishing Company, The Netherlands, 2003.
- [13] H.F. Brito, O.L. Malta, M.C.F.C. Felinto, E.E.S. Teotonio, in: J. Zabicky (Ed.), *The Chemistry of Metal Enolate*, John Wiley & Sons, Chichester, England, 2009.
- [14] J.-M. Lehn, *Angew. Chem. Int. Ed. Engl.* 29 (1990) 1304.
- [15] X.M. Guo, L.S. Fu, H.J. Zhang, L.D. Carlos, C.Y. Peng, J.F. Guo, J.B. Yu, R.P. Deng, L. N. Sun, *New J. Chem.* 29 (2005) 1351.
- [16] K. Binnemans, *Chem. Rev.* 109 (2009) 4283.
- [17] K. Inoue, K. Ohto, K. Yoshizuka, T. Yamaguchi, T. Tanaka, *Bull. Chem. Soc. Jpn.* 70 (1997) 2443.
- [18] E. Repo, J.K. Warchol, T.A. Kurniawan, M.E.T. Sillanpää, *Chem. Eng. J.* 161 (2010) 73.
- [19] M. Hughes, E. Rosenberg, *Sep. Sci. Technol.* 42 (2007) 261.
- [20] L. Wang, L. Yang, Y. Li, Y. Zhanga, X. Ma, Z. Ye, *Chem. Eng. J.* 163 (2010) 364.
- [21] L.Q. Yang, Y.F. Li, L.Y. Wang, Y. Zhang, X.J. Ma, Z.F. Ye, *J. Hazard. Mater.* 180 (2010) 98.
- [22] R. Kumar, M.A. Barakat, Y.A. Daza, H.L. Woodcock, J.N. Kuhn, *J. Colloid Interf. Sci.* 408 (2013) 200.
- [23] E. Repo, J.K. Warchol, A. Bhatnagar, M. Sillanpää, *J. Colloid Interface Sci.* 358 (2011) 261.
- [24] L. Lattuada, A. Barge, G. Cravotto, G.B. Giovenzana, L. Tei, *Chem. Soc. Rev.* 40 (2011) 3019.
- [25] E. Repo, T.A. Kurniawan, J.K. Warchol, M.E.T. Sillanpää, *J. Hazard. Mater.* 171 (2009) 1071.
- [26] T.J. Wenzel, R. Evertsen, B.E. Perrins, T.B. Light Jr., A.C. Bean, *Anal. Chem.* 70 (1998) 2085.
- [27] Y.Y. Li, B. Yan, Q.P. Li, *Dalton Trans.* 42 (2013) 1678.
- [28] E. Fadeyev, S. Smola, O. Snurnikova, O. Korovin, N. Rusakova, *J. Sol–Gel Sci. Technol.* 68 (2013) 479.
- [29] B. Liu, J. Gao, J. Wang, Y.F. Wang, R. Xu, P. Hu, L.Q. Zhang, X.D. Zhang, *Russ. J. Coord. Chem.* 35 (2009) 422.
- [30] X. Chen, D. Li, J. Wang, B. Liu, Y. Kong, D. Wang, X.D. Zhang, *J. Coord. Chem.* 63 (2010) 3897.
- [31] J.Q. Gao, T. Wu, J. Wang, X.D. Jin, D. Li, B.X. Wang, K. Li, Y. Li, *Russ. J. Coord. Chem.* 37 (2011) 817.
- [32] Y. Wang, Y. Yue, H. Li, Q. Zhao, Y. Fang, P. Cao, *Photochem. Photobiol. Sci.* 10 (2011) 128.
- [33] M.P. Bemquerer, C. Bloch, H.F. Brito, E.E.S. Teotonio, M.T.M. Miranda, *J. Inorg. Biochem.* 91 (2002) 363.
- [34] N. Arsalani, S.Z. Mousavi, *Irn. Polym. J.* 12 (2003) 291.
- [35] T. Takeshita, T. Shimohara, S. Maeda, *J. Am. Oil Chem. Soc.* 59 (1982) 104.
- [36] M. Waseem, S. Mustafa, A. Naeem, G.J.M. Koper, K.H. Shah, *Desalination* 277 (2011) 221.
- [37] D.L. Vien, N.B. Colthup, W.G. Fateley, J.G. Grasselli, *The Handbook of Infrared and Raman Characteristic Frequencies of Organic Molecules*, Academic Press, San Diego, California, USA, 1991.
- [38] Y. Ma, H. Wang, W. Liu, Q. Wang, J. Xu, Y. Tang, *J. Phys. Chem. B* 113 (2009) 14139.
- [39] B.E. Yoldas, *J. Mater. Res.* 5 (1990) 1157.
- [40] J. Garcia, M. Mondragon, C. Tellez, *Mater. Chem. Phys.* 41 (1995) 15.
- [41] W.H. Green, K.P. Le, J. Grey, T.T. Au, M.J. Sailor, *Science* 276 (1997) 1826.
- [42] T. Brankova, V. Bekiari, P. Lianos, *Chem. Mater.* 15 (2003) 1855.
- [43] L.D. Carlos, R.A.S. Ferreira, R.N. Pereira, M. Assunção, V.Z. Bermudez, *J. Phys. Chem. B* 108 (2004) 14924.
- [44] S. Sato, M. Wada, *Bull. Chem. Soc. Jpn.* 43 (1970) 1955.
- [45] G.F. Sá, O.L. Malta, C.M. Donegá, A.M. Simas, R.L. Longo, P.A. Santa-Cruz, E. F. Silva Jr, *Coord. Chem. Rev.* 196 (2000) 165.
- [46] W.T. Carnall, H. Crosswithe, H.M. Crosswithe, *Energy Level Structure and Transition Probabilities of the Trivalent Lanthanide in LaF₃*, Argonne National Lab, Argonne Illinois, 1977.
- [47] H. Wang, Y. Ma, H. Tian, N. Tang, W. Liu, Q. Wang, Y. Tang, *Dalton Trans.* (39, 2010) 7485.
- [48] E.E.S. Teotonio, M.C.F.C. Felinto, H.F. Brito, O.L. Malta, A.C. Trindade, R. Najjar, W. Streck, *Inorg. Chim. Acta* 357 (2004) 451.
- [49] E.R. Souza, I.G.N. Silva, E.E.S. Teotonio, M.C.F.C. Felinto, H.F. Brito, *J. Lumin.* 130 (2010) 283.
- [50] Y. Uno, *Electroluminescent Display*, World Scientific Publishing Co. Pte. Ltd., Singapore, 1995.